European Heart Journal (2006) **27**, 2459–2467
doi:10.1093/eurheartj/ehl255

Postmortem unenhanced magnetic resonance imaging of myocardial infarction in correlation to histological infarction age characterization

Christian Jackowski[1]*, Andreas Christe[1,2], Martin Sonnenschein[3], Emin Aghayev[1], and Michael J. Thali[1]

[1] *Centre of Forensic Imaging and Virtopsy, Institute of Forensic Medicine, University of Bern, IRM—Bühlstrasse 20, CH-3012 Bern, Switzerland;* [2] *Institute of Diagnostic Radiology, Inselspital, University of Bern, 3010 Bern, Switzerland; and* [3] *Department of Diagnostic Radiology, Sonnenhof Spital AG, Buchserstrasse 30, 3006 Bern, Switzerland*

Received 13 April 2006; revised 6 August 2006; accepted 31 August 2006; online publish-ahead-of-print 14 September 2006

KEYWORDS
Virtopsy;
Magnetic resonance imaging;
Postmortem cardiac imaging;
Myocardial infarction;
Virtual autopsy

Aims Postmortem magnetic resonance (MRI) imaging is currently evaluated as alternative to traditional autopsy and myocardial infarction plays a key role therein. The aim of this study is to determine the suitability of postmortem MRI in infarction age staging.
Methods and results In eight human forensic corpses presenting with a total of 11 myocardial infarcted areas, short-axis, transversal, and longitudinal long-axis images (T1, T2, stir, flair) were acquired *in situ* on a 1.5 T system. During subsequent autopsy, the section technique was adapted to short-axis images. Histological investigations were performed along the entire circumference of the left ventricle to correlate the signal alteration in MR to the histological appearance. Two peracute infarctions were not detected in MRI and autopsy. Four acute infarcted areas presented with decreased signal in necrotic centres and increased signal in marginal myocardial regions (T2-weighted). T1-weighted images showed local hyperintensities when intramyocardial haemorrhage occurred. Four cases showed subacute infarctions with hyperintense regions in T2-weighted images and no signal alteration in T1-weighted images. Four chronic myocardial infarctions showed distinctively decreased signals in all applied sequences.
Conclusion Postmortem MRI demonstrates myocardial infarction *in situ* and allows for an infarction age estimation based on the signal behaviour.

Introduction

Postmortem imaging is being evaluated and validated to assess different causes of death in a minimally invasive manner. This is thought to serve as a future alternative to traditional autopsy in suitable cases in order to antagonize the reduction of postmortem diagnostics due to decreasing autopsy rates.[1,2] Benefits such as the reduction of the emotional strain of relatives of the deceased as well as results of postmortem cross-sectional imaging in different injuries and diseases have already been described.[3–9] Only two studies concentrated on the postmortem cross-sectional findings of the heart and showed exemplarily that myocardial infarction is also detectable in postmortem magnetic resonance imaging (MRI).[10,11] Until today, no aimed study investigated the appearances of different infarction ages in postmortem MRI.

As cardiac deaths represent the major portion of natural deaths in the first world, it is of particular importance that postmortem imaging can detect pathologies of the human heart. Macromorphological alterations such as hypertrophy or dilatation are less challenging in this context than the tissue alterations occurring during and after cardiac ischaemia.[10] However, as these are the most prevalent causes for cardiac deaths, regardless of insufficiency or arrhythmia, these tissue alterations have to be detected by postmortem imaging. As shown in previous studies,[10,12] multislice computed tomography (MSCT) is an excellent tool for the detection of coronary calcifications, also postmortem, but fails in assessing critical tissue alterations of the myocardium. However, MRI can close this gap.[3,10,11] It is already known that myocardial infarction as well as collagenous myocardial scarring can be visualized in predominantly T2-weighted MRI sequences. Regarding the forensic importance of this issue, further questions need to be answered. Is early (peracute) myocardial infarction detection possible using postmortem MRI, which has been a challenge in traditional autopsy since decades?[13–15] Are there sequences that allow an improved assessment of myocardial infarction in postmortem imaging compared with the usually used T2-weighted sequences?

* Corresponding author. Tel: +41 316318412; fax: +41 316313833.
E-mail address: christian.jackowski@irm.unibe.ch

Table 1 Case characteristics

	Sex	Age	PMI (h)	Clinical age of infarction	Histological staging	Localization	Comments
1	Female	51	17	6 days	(Acute) and (Subacute)	inf + lat	
2	Male	53	14	8 weeks	(Acute) and (Chronic)	lat + inf	
3	Female	52	12	<6	(Peracute)	ant/sep	Acute LAD occlusion
4	Male	62	50	<1 h	(Peracute)	lat	Acute CX occlusion, ECG documentation
5	Male	71	22	2–3 days	(Acute) and (Chronic)	inf + ant	
6	Male	44	24	Varying	(Acute/subacute/chronic)	Global	Cor bovinum (uraemic)
7	Male	71	26	—	(Subacute)	lat/inf	
8	Male	57	10 years	10 years	(Subacute/chronic)	sep	

PMI indicates the postmortem interval as time from death to scanning; inf, inferior; lat, lateral; ant, anterior; sep, septal; LAD, left anterior descending coronary artery; CX, circumflex coronary artery; staging in brackets indicates a local combined occurrence.

To address these questions, different stages of myocardial infarction, with different postmortem intervals (PMI), have to be investigated and a correlation to the histological alterations within the myocardium has to be performed under consideration of the particular case histories. This is intended to create a time course of the postmortem imaging appearances of myocardial infarction similar to histological time courses already compiled several decades ago.[16,17]

First immunohistochemical signs of myocardial infarction become visible after 2–4 h survival time. Ischaemia results in an early global acidosis (pH < 6.9) due to the consumption of the ATP.[18] Thereby, the ischaemic myocytes become increasingly susceptible to eosinophilic stains as a first visible sign in routine histology. In this timeframe, the occurrence of contraction band necrosis can be observed.[19] Single fibres or small groups of fibres show already a loss of striation, are swollen (cellular oedema), or thin and wavy.[16,20] Usually there is a small subendocardial layer (0.3–0.5 mm) of surviving tissue, which is explained by an assumed oxygen diffusion through the endocardium.[17,20] Thereby, in two situations such as intraventricular thrombi covering the endocardium and pathologically thickened endocardium, no surviving subendocardial layer can be expected.[21] As a frequent finding, haemorrhages occur focally within the infarcted tissue. The inflammatory reaction is commenced by the infiltration of polymorphonuclear leucocytes. The amount of infiltration increases progressively up to the fourth day. After the fifth day, the polymorphonuclear leucocytes become necrotic and begin to disappear. Simultaneously, mononuclear cells start the removal of the necrotic muscle by phagocytosis. Newly formed blood capillaries can be found, which start growing into the infarcted regions from the periphery to the ischaemic centre. Along these ingrowing vessels, fibroblasts reach the necrotic areas. The fibroblasts (today called fibroblast-like cells or myofibroblasts, as they express alpha-smooth muscle actin) start the formation of collagen (types I and III).[17,22–24] The formation of collagen is moderately prominent at 3 weeks and reaches its maximum at about 3 months. This fibrous tissue reaction also encroaches non-infarcted myocardial regions but to a distinctively lesser extent.[25–27] These ongoing alterations seem only to be influenceable by an early revascularization during the first 4–6 h after the coronary occlusion, resulting in a reduction of the infarct size but not in a complete reversibility.[28,29] Later, reperfusion does not influence the ongoing necrosis but accelerates subsequent inflammatory and remodelling reactions.

The aim of this study is to correlate MRI appearances of myocardial infarction to the macroscopic as well as the histological appearance in order to estimate the age of the infarction based on the MR images.

Methods

The study was approved by the local Ethics Committee.

Eight cases from the Virtopsy® project, which presented with myocardial infarction as cause of death, were included (*Table 1*). Eleven separately infarcted areas to be investigated were distributed within these eight cases. General full body scanning procedures and issues of logistics, costs, and used equipment have been described in detail in previous publications.[3,10,30] Additional to the thoracic scanning methods, the hearts of the investigated bodies were scanned using sequences that have been adopted as follows: short-axis, vertical, and horizontal long-axis images have been acquired using conventional clinical-used localizer settings;[31] T1-weighted (TE 15 ms, TR 400 ms) 2 mm slice thickness; T2-weighted (TE 96 ms, TR 4 s) 2 mm slice thickness (with and without fat saturation); stir (TE 14 ms, TI 133 ms, TR 3 s) 3 mm slice thickness; and flair (TE 217.5 ms, TI 2200 ms, TR 11002 ms) 3 mm slice thickness.

Histological correlation was performed after histological specimens of the entire circumference of the left ventricle, according to the short-axis MR images, were prepared. Histological stains included haematoxylin and eosin (H&E), van Gieson, and chromotrop-aniline-blue (CAB). The coronary orifices and the apex were used as anatomical landmarks that allowed comparing similar slice sections in imaging and autopsy. Histological grading was performed according to *Table 2* from peracute, acute (early and late), subacute (early and late), and chronic infarctions.

The appendant antemortem anamneses have been examined to assess subjective or objective signs for the time point of onset, and combined with the histological age staging, the age of the ischaemia was determined.

Results

Table 2 displays the data of the included eight cases. Two cases showed no myocardial morphological signs of ischaemia (peracute), although an indicative anamnesis was present and an acute coronary occlusion could be found at autopsy. Four cases showed acutely infarcted regions, four

Table 2 Histological and MRI correlation

Case			1		2		3	4	5		6	7	8
Localization			inf	lat	inf	lat	ant/sep	lat	inf	ant	Global	lat/inf	sep
Peracute							x	x					
Acute	Early acute	Increased eosinophilia	x		x				x		x		
		Wavy fibres			x				x		x		
		Oedema	x		x				x		x		
		Contraction bands	x		x				x				
		Myocardial haemorrhage			x				x				
	Late acute	Neutrophiles infiltration	x		x				x				
		Fibre necrosis	x		x				x				
Subacute	Early subacute	Macrophages infiltration									x	x	
		Fibroblasts									x	x	
	Late subacute	Fibroblasts/fibrocytes		x							x	x	x
		Loose connective tissue		x							x	x	x
		Angiogenesis		x								x	x
Chronic		Fibrocytes				x				x	x		x
		Collageneous scar				x				x	x		x
		Hypertrophic adjacent fibres				x				x	x		x
MRI signal	T1		cen 0 mar ↓	0	cen 0 mar ↓	↓	0	0	Basal/apical 0 Near rupture ↑	↓	0	0	↓↓
	T2		cen ↓↓ mar ↑↑	↑↑	cen ↓↓ mar ↑↑	↓	0	0	cen ↓↓ mar ↑↑	↓	Varying	↑↑	↓↓
	T2 fat saturation		cen ↓↓ mar ↑↑	↑↑	cen ↓↓ mar ↑↑	↓	0	0	cen ↓↓ mar ↑↑	↓	Varying	↑↑	↓↓
	Stir		cen ↓↓ mar ↑↑	↑↑	cen ↓↓ mar ↑↑	↓	0	0	cen ↓↓ mar ↑↑	↓	Varying	↑↑	↓↓
	Flair		cen ↓ mar ↑	↑	cen ↓ mar ↑	↓	0	0	cen ↓ mar ↑	↓	Varying	↑	↓↓

x indicates the histological occurrence of the finding; cen, central; mar, marginal; 0, no signal alteration visible; ↑, slight increase in signal; ↑↑, distinctive increase in signal; ↓, slight decrease in signal; ↓↓ distinctive decrease in signal.

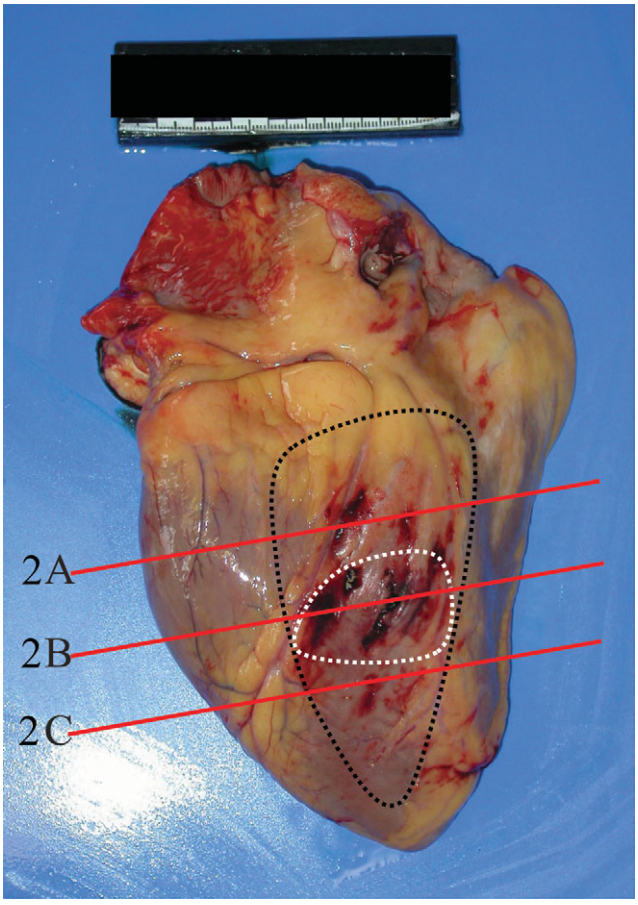

Figure 1 Autopsy photograph showing the posterior view of the heart in case 5. Note several minor and one major (transmural) rupture in the pale posterior wall. General extension of the infarction is indicated by the black dotted line, the extension of haemorrhagic myocardium is given by the white dotted line and red lines (*A–C*) indicate the level of the short-axis images in *Figure 2*.

cases showed subacute infarcted regions, and four cases showed chronic infarction (combinations occurred).

Peracute ischaemia with subsequent death showed no assessable myocardial alteration in MRI or autopsy and histology. A fresh coronary occlusion was found to have caused death in these two cases.

Acute ischaemia (*Figures 1* and *2*) with histological central necrosis, peripheral oedema, and cellular reactions showed two different areas of signal behaviour. A signal reduction within the necrotic centre of the myocardial wall in T2-weighted, stir, and flair sequences was present. Predominantly, subepicardial marginal regions showed increased signals in T2-weighted, stir, and flair sequences. T1-weighted imaging failed to show distinctive signal alterations in the affected myocardial regions. Intramyocardial postinfarction haemorrhage caused the signal of T1-weighted images to increase slightly.

Subacute ischaemia (*Figure 3*), histologically characterized by fibroblasts that form loose connective tissue replacing the necrotic fibres and ingrowing vessels, showed increased signals in T2-weighted, stir, and flair images. T1-weighted images failed to show signal alterations in these regions.

Chronic infarction (*Figure 4*) with definite collagen formation at histology showed a signal loss in all applied sequences, with distinctiveness decreasing from T2 to stir to flair to T1.

Figure 5 gives the time course of MRI signals in postmortem MRI of myocardial infarction based on the investigated cases.

Discussion

The rapid further development of the modern cross-sectional technique MRI already enabled its use in clinical routine to image structural changes within ischaemic myocardial tissue. Although motion artifacts aggravate diagnostics because of cardiac motion or respiration, clinical radiology has the advantage of contrast enhancing agent application, using the blood flow for its distribution. Thereby, the characteristics of enhancement are used to assess the size and age of the ischaemia.[32] In postmortem cardiac imaging, not yet having the possibility to assess late enhancements, this disadvantage seems to be caught up by the excellent image quality due to the absence of any cardiac motion or breathing-related artifacts. Nevertheless, already in the early eighties, unenhanced clinical MRI also showed promising results for the identification of myocardial infarction, using the significant increase in the water content (oedema) within the infarcted muscle.[33,34] These early studies as well as following ones showed that there is a significant prolongation of the T2-relaxation time within the infarcted myocardium.[35–38] T1-relaxation time was likewise prolonged, but to a lesser extent.[37,38] Thereby, the image contrast was greatest on T2-weighted images.[37] This is so far in absolute concordance to our previously published results where we also stated that the contrast in myocardial infarction images was greatest in T2-weighted images.[10] Although the clinical cardiac MRI in recent years implements different contrast agents, application schedules as well as contrast agent and cardiac motion adapted sequences to assess cardiac pathology,[39–42] postmortem cardiac MRI still depends on the imaging of the unenhanced structural alterations that occurred during the different stages of myocardial infarction.

Our results show that in peracute infarction, both autopsy and imaging failed to visualize myocardial changes. This is caused by the lacking survival time that would allow for vital reactions within the myocardium, such as oedema, necrosis, and so on. When ischaemia and death of the individual occur in close succession, these reactions are not possible anymore. Even autopsy and routine histology fail to discriminate between initial ischaemic myocardium and subsequent death with then 'global ischaemic' myocardium. In these cases, one still depends on coronary diagnostics showing stenosis or occlusions. Unfortunately, only half of these peracute cases present with an acute coronary lesion.[43] The remaining cases present with extra-cardiac signs of cardiac failure, but no pathological cardiac findings. If the 3 T scanners become more widespread, the higher resolution (matrix 1024×1024) might allow for the detection of smaller, for example, oedematous myocardial alterations that can easily be overseen at autopsy but can nonetheless induce arrhythmias.

Furthermore, recent research efforts concentrate on the possibilities of increasing the significance of postmortem imaging by an application of postmortem contrast agents.[12,44] As already shown in porcine *ex vivo* experiments,

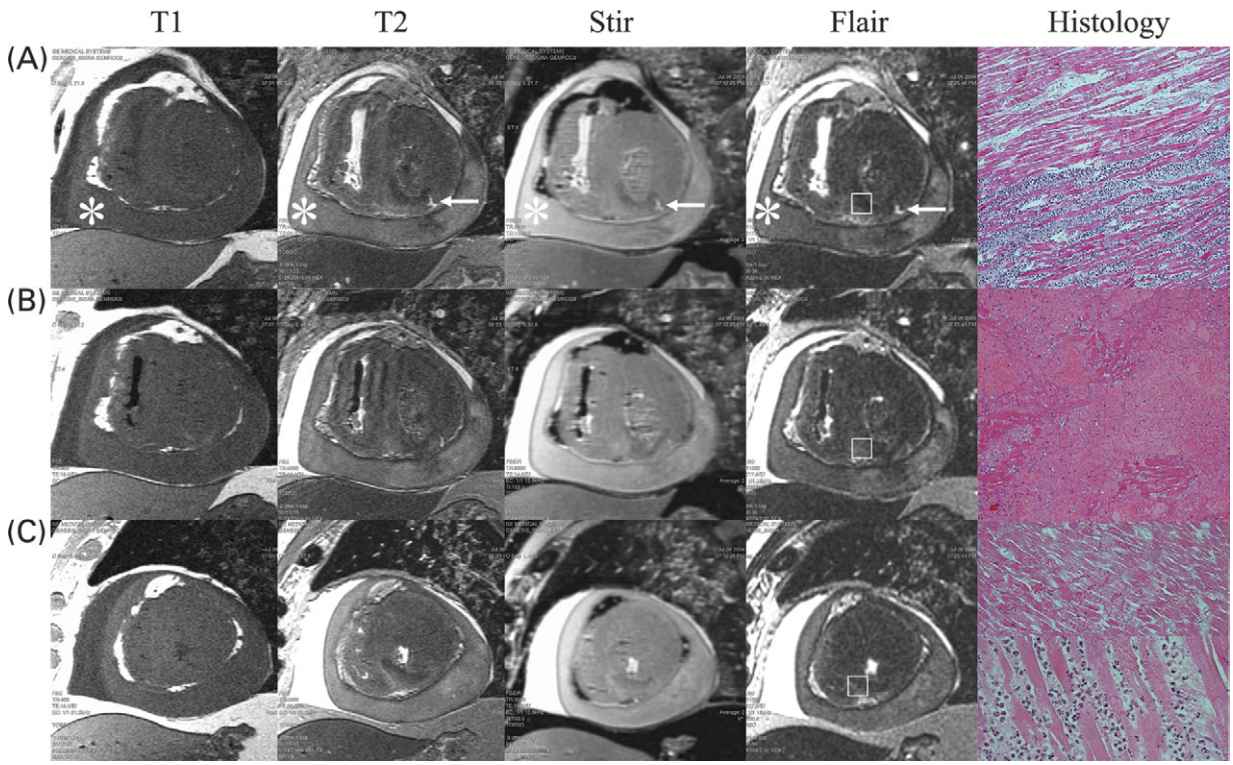

Figure 2 Acute myocardial infarction (case 5) in postmortem MRI. Short-axis images as indicated in *Figure 1* show two different MRI and histological appearances. The basal and apical planes (*A* and *C*) show no obvious signal alteration in T1-weighted images. T2-weighted, stir, and flair (less distinctive) images present with a central signal decrease and increasing signal surrounding the hypointensity. This hyperintense margin is more noticeable on the epicardial margin (small rectangles indicate the origin of the appendant histological specimen). Histological appearance is dominated by a necrotic centre of the lesion with eosinophilic fibres without nuclei and contraction band necrosis surrounded by oedematous myocardium and infiltrating leucocytes. In contrast, the middle images (*B*) show local signal increasing within the T1 image. Histology demonstrates broad intramural haemorrhage within the necrosis. Note the pericardial tamponade (∗) obvious in all images because of the transmural rupture (*A*) (arrow).

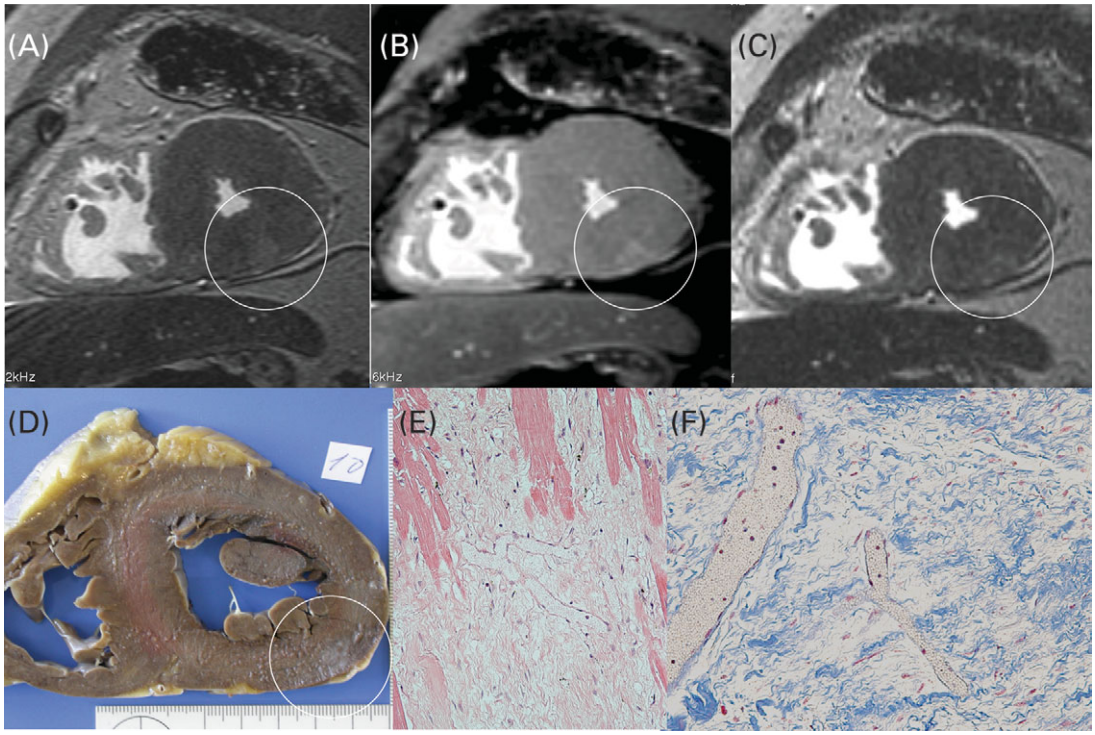

Figure 3 Subacute myocardial infarction (case 7) in postmortem MRI. Short-axis images [(*A*) T2, (*B*) stir, and (*C*) flair] show a local hyperintensity within the posterior/lateral wall well correlating to the appearance of the local subacute subepicardial infarcted area at autopsy (*D*). Histology [(*E*) H&E, (*F*) CAB)] shows loose connective tissue formation and angiogenesis as the reason for the signal increase in T2-weighted sequences.

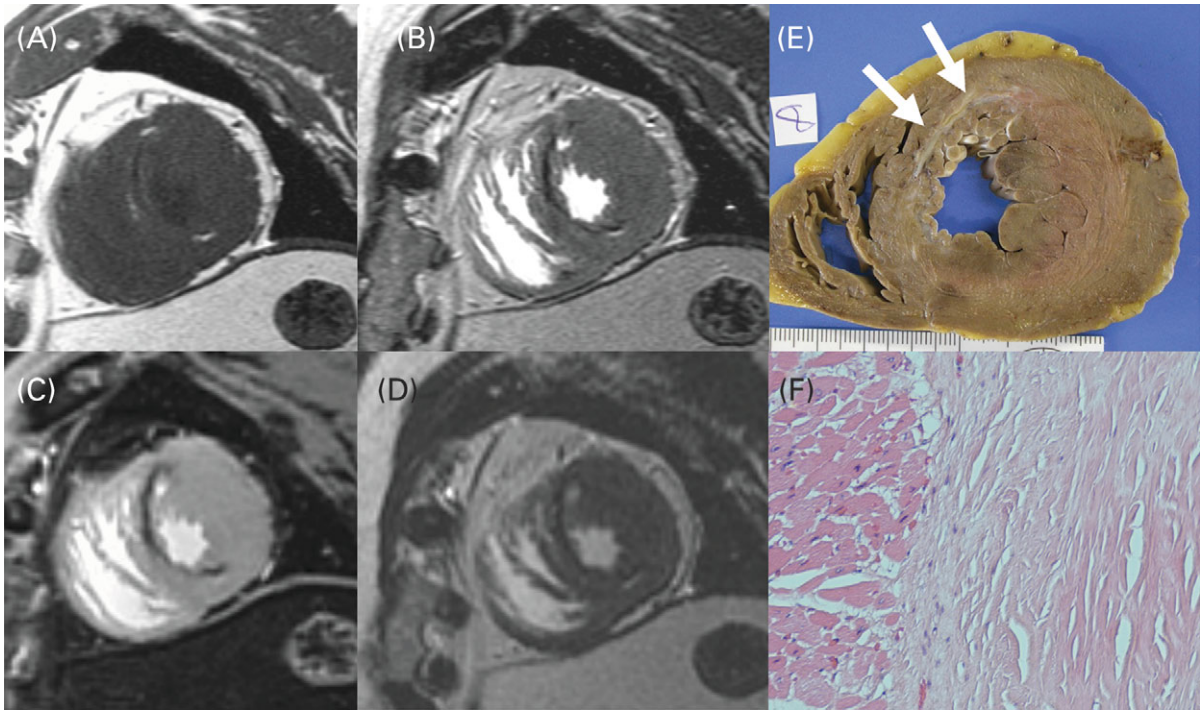

Figure 4 Chronic myocardial infarction (case 8) in postmortem MRI. Short-axis images [(*A*) T1, (*B*) T2, (*C*) stir, and (*D*) flair] show broad decrease in signal along the septum with thinning of the septal wall. Autopsy (*E*) demonstrates definite collagenous transformation of the infarcted septal myocardium with scar-caused shrinking of the septal diameter. Histology (*F*) at the border between scar and vital myocardium shows cell-free collagene (right) as the cause for the significant decrease of signal in MRI.

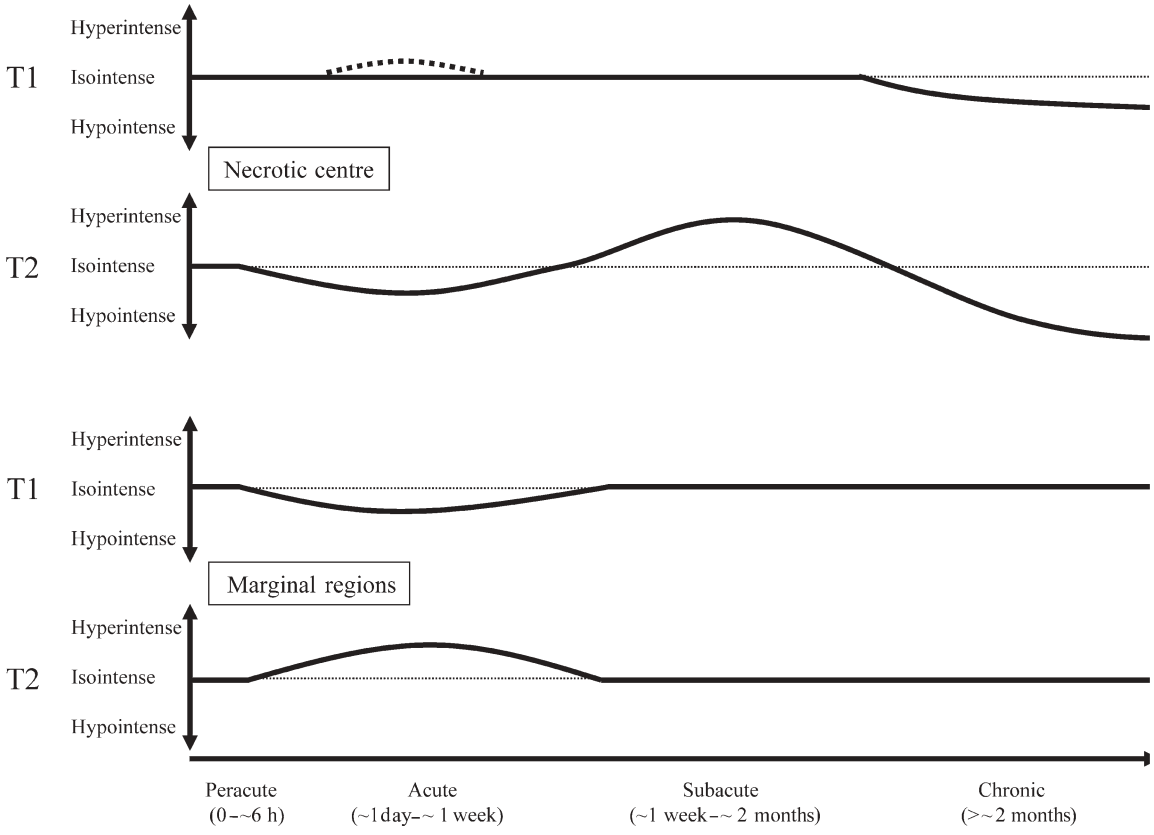

Figure 5 Time course of MR signal in postmortem MRI of myocardial infarction. T1 and T2 signal course within the necrotic centre (upper graphs) and in marginal myocardial regions (lower graphs). Dashed line at the T1 graph of the necrotic centre indicates the signal increase if intramural haemorrhage occurs. Signal course of stir and flair sequences behaves similar to T2 but in distinctively lesser amplitudes.

distribution defects of injected gadolinium could be simulated within the porcine myocardium.[12] Minimal invasively applied, this would allow for dealing with these forensic cases in a minimal invasive manner if necessary.

Acute infarction showed decreased signals in T2-weighted, stir, and flair sequences in central areas correlating to the necrotic zone within the infarcted area. This might be a result of the hypoperfusion that led to fewer protons within these tissue regions (hypothesis). Oedema and cellular reactions starting from peripheral regions caused the signals in T2-weighted, stir, and flair images to be higher in marginal parts of the ischaemic lesion. The proportion of necrotic central signal decrease to reactive marginal signal increase might be a useful hint for a more detailed estimation of the survival time in acute lesions. Of course, this needs to be investigated in a larger population of acute infarction cases. Postinfarction intramyocardial haemorrhage was the only histological finding that accompanied an increasing signal in T1-weighted images. Therefore, hyperintensities within T1-weighted images in regions that show infarction signs in T2-weighted images are strongly indicative for intramyocardial haemorrhage.

Subacute and chronic infarctions reach forensic importance as a cause of death due to a continuous reduction of the ejection fraction leading to acute cardiac insufficiency or by generating a lethal ventricular tachycardia. Thereby, these findings are essential in ~40% of cardiac deaths when extra-cardiac findings such as congested internal organs indicate a cardiac failure as cause of death, but acute ischaemic myocardial findings are missing.[43] These stages can now also be differentiated by the signal behaviour in predominantly T2-weighted sequences.

Besides contrast agent injection as a promising adjuvant technique supporting postmortem imaging, diffusion weighted cardiac imaging might allow for imaging of fibre alterations, especially wavy fibres in early acute stages.[45–48]

We are convinced that postmortem cross-sectional imaging can serve as an alternative investigation tool when traditional autopsy is refused for different reasons. One major function of forensic medicine is to discriminate natural from non-natural deaths. To establish a minimal invasive postmortem imaging procedure as an alternative to traditional autopsy, postmortem cross-sectional imaging must be able to serve as a tool for assessing macromorphological changes and be able to replace the naked eye in a traditional autopsy. It is therefore thought to act similar to the eye of the forensic pathologist as a detection tool for local macro-pathological alterations and may allow an initial diagnosis but will normally depend on histological confirmation. Tissue specimen of pathological areas can be obtained using an image-guided biopsy technique,[49] and coronary diagnostics can be performed using minimal invasive postmortem angiography techniques available today.[12,44] As these angiography techniques are implemented on the basis of MSCT, a minimal invasive case management will deserve a combination of both cross-section techniques as described in the virtopsy idea.[3] Especially, peracute infarction cases depend on angiographic coronary diagnostics to visualize stenotic alterations or occlusions.

Obviously, the major limitation of the presented study is the low number of included myocardial infarction cases. As a forensic institution predominantly investigating homicides, suicides, accidents, and deaths that occurred under unclear circumstances, the very common cardiac death due to myocardial infarction is not that common in forensic case material. Close collaborations with pathological institutes or cardiological clinics could result in a larger study population. Since the first CT and MR scanners have already been installed in forensic institutes (Copenhagen, Melbourne, and Bern), further studies become possible with less logistic efforts in the near future.

There are physiological postmortem alterations within the human myocardial tissue, which interact with the signal behaviour in MRI. Cessation of the circulation results in sedimentation of cellular blood components not only within the major vessels but also within the tissue of different organs including the myocardium.[50] These so-called internal livores can cause hypointense areas (T2-weighted imaging) in dependant myocardial regions, which should not be misinterpreted as a postischaemic lesion. As a second postmortem feature influencing the imaging appearance, rigor mortis needs to be mentioned. Similar to the rigor mortis within the skeletal musculature, the heart remains in a systolic situation when ATP reserves of the myocardium are exhausted. Being a ring muscle, this leads to an increase in intramyocardial pressure reaching from subepicardial to subendocardial regions. Thereby, interstitial fluids arrange in less-pressured subepicardial regions and cause a signal decline from subepicardial to subendocardial regions when the rigor mortis is at its maximum (PMI 24–48 h) or the myocardium is hypertrophic. This phenomenon is slightly visible in the hypertrophic lateral wall of case 8 as shown in *Figure 4B*. The third postmortem finding influencing MRI is a gas accumulation within the cardiac cavities due to either gas embolism or beginning putrefaction. These gas bubbles can cause imaging artefacts as occurred in the septum of the T2-weighted image in *Figure 2B* due to the gas within the right ventricle. Since human corpses do not retain the vital body temperature, postmortem MRI needs to define adapted scanning parameters. Forensic corpses have core temperatures normally ranging from 4 to 30°C (with several exceptions such as burned or frozen corpses); therefore, there is a need to define new echo, inversion, and repetition times for closer temperature ranges that intend to increase the signal- and contrast-to-noise ratios in postmortem MR images. This is going to be addressed in an upcoming study of our group.

To our knowledge, there are no experiences with other myocardial alterations such as myocarditis in postmortem MRI until today. Potential differential diagnoses need to be addressed in specific future studies to define their postmortem imaging appearance. As long as the postmortem diagnosis in forensic medicine is based on a combination of imaging and image-guided biopsy with histological investigation, there is no risk for misinterpretation of images.

The results of the presented study demonstrate that postmortem-unenhanced MRI is able to visualize and discriminate the different stages of myocardial infarction. Thereby, it can serve—combined with minimal invasive angiography and biopsy techniques—as a future alternative to traditional autopsy in selected cases.

Acknowledgements

We are grateful to Urs Königsdorfer, Roland Dorn, and Therese Perinat for their experienced assistance at autopsy and preparation

of the histological specimen. The authors thank Stephan Bolliger for the support during manuscript preparation and Karin Zwygart as well as Verena Beutler (both radiological technicians) for their motivated commitment at scanning during the evening hours.

Conflict of interest: none declared.

References

1. Sinard JH. Factors affecting autopsy rates, autopsy request rates, and autopsy findings at a large academic medical center. *Exp Mol Pathol* 2001;**70**:333–343.
2. Ward HE, Clarke BE, Zimmerman PV, Cleary MI. The decline in hospital autopsy rates in 2001. *Med J Aust* 2002;**176**:91.
3. Thali MJ, Yen K, Schweitzer W, Vock P, Boesch C, Ozdoba C, Schroth G, Ith M, Sonnenschein M, Doernhoefer T, Scheurer E, Plattner T, Dirnhofer R. Virtopsy, a new imaging horizon in forensic pathology: virtual autopsy by postmortem multislice computed tomography (MSCT) and magnetic resonance imaging (MRI)—a feasibility study. *J Forensic Sci* 2003;**48**:386–403.
4. **http://www.virtopsy.com (2006)**.
5. Aghayev E, Yen K, Sonnenschein M, Ozdoba C, Thali M, Jackowski C, Dirnhofer R. Virtopsy post-mortem multi-slice computed tomograhy (MSCT) and magnetic resonance imaging (MRI) demonstrating descending tonsillar herniation: comparison to clinical studies. *Neuroradiology* 2004;**46**:559–564.
6. Thali M, Vock P. Role of and Techniques in Forensic Imaging. In: Payen-James J, Busuttil A, Smock W, ed. *Forensic Medicine: Clinical and Pathological Aspects*. London: Greenwich Medical Media; 2003. p731–745.
7. Jackowski C, Thali M, Sonnenschein M, Aghayev E, Yen K, Dirnhofer R, Vock P. Visualization and quantification of air embolism structure by processing postmortem MSCT data. *J Forensic Sci* 2004;**49**:1339–1342.
8. Thali MJ, Yen K, Plattner T, Schweitzer W, Vock P, Ozdoba C, Dirnhofer R. Charred body: virtual autopsy with multi-slice computed tomography and magnetic resonance imaging. *J Forensic Sci* 2002;**47**:1326–1331.
9. Thali MJ, Yen K, Schweitzer W, Vock P, Ozdoba C, Dirnhofer R. Into the decomposed body-forensic digital autopsy using multislice-computed tomography. *Forensic Sci Int* 2003;**134**:109–114.
10. Jackowski C, Schweitzer W, Thali M, Yen K, Aghayev E, Sonnenschein M, Vock P, Dirnhofer R. Virtopsy: postmortem imaging of the human heart *in situ* using MSCT and MRI. *Forensic Sci Int* 2005;**149**:11–23.
11. Jachau K, Heinrichs T, Kuchheuser W, Krause D, Wittig H, Schoening R, Beck N, Beuing O, Doehring W, Jackowski C. Computed tomography and magnetic resonance imaging compared to pathoanatomic findings in isolated human autopsy hearts. *Rechtsmedizin* 2004;**14**:109–116.
12. Jackowski C, Sonnenschein M, Thali MJ, Aghayev E, von Allmen G, Yen K, Dirnhofer R, Vock P. Virtopsy: postmortem minimally invasive angiography using cross section techniques—implementation and preliminary results. *J Forensic Sci* 2005;**50**:1175–1186.
13. Varga M, Zsonda L. A simple method for postmortem detection of acute myocardial infarction. *Forensic Sci Int* 1988;**37**:259–263.
14. Hansen SH, Rossen K. Evaluation of cardiac troponin I immunoreaction in autopsy hearts: a possible marker of early myocardial infarction. *Forensic Sci Int* 1999;**99**:189–196.
15. Ribeiro-Silva A, CC SM, Rossi MA. Is immunohistochemistry a useful tool in the postmortem recognition of myocardial hypoxia in human tissue with no morphological evidence of necrosis? *Am J Forensic Med Pathol* 2002;**23**:72–77.
16. Fishbein MC, Maclean D, Maroko PR. The histopathologic evolution of myocardial infarction. *Chest* 1978;**73**:843–849.
17. Mallory GK, White PD, Salcedo-Salgar J. The speed of healing of myocardial infarction—a study of the pathologic anatomy in seventy-two cases. *Am Heart J* 1939;**18**:647–671.
18. Walpoth BH, Galdikas J, Tschopp A, Vorburger T, Lazeyras F, Schaffner T, Althaus U. Differentiation of cardiac ischemia and rejection by nuclear magnetic spectroscopy. *Thorac Cardiovasc Surg* 1991;**39**(Suppl. 3): 217–220.
19. Baroldi G, Mittleman RE, Parolini M, Silver MD, Fineschi V, Myocardial contraction bands. Definition, quantification and significance in forensic pathology. *Int J Legal Med* 2001;**115**:142–151.
20. Fishbein MC, Maclean D, Maroko PR. Experimental myocardial infarction in the rat: qualitative and quantitative changes during pathologic evolution. *Am J Pathol* 1978;**90**:57–70.
21. Bouchardy B, Majno G. Histopathology of early myocardial infarcts. A new approach. *Am J Pathol* 1974;**74**:301–330.
22. Sun Y, Weber KT. Infarct scar: a dynamic tissue. *Cardiovasc Res* 2000;**46**:250–256.
23. Morales C, Gonzalez GE, Rodriguez M, Bertolasi CA, Gelpi RJ. Histopathologic time course of myocardial infarct in rabbit hearts. *Cardiovasc Pathol* 2002;**11**:339–345.
24. Virag JI, Murry CE. Myofibroblast and endothelial cell proliferation during murine myocardial infarct repair. *Am J Pathol* 2003;**163**:2433–2440.
25. Volders PG, Willems IE, Cleutjens JP, Arends JW, Havenith MG, Daemen MJ. Interstitial collagen is increased in the non-infarcted human myocardium after myocardial infarction. *J Mol Cell Cardiol* 1993; **25**:1317–1323.
26. Litwin SE, Litwin CM, Raya TE, Warner AL, Goldman S. Contractility and stiffness of noninfarcted myocardium after coronary ligation in rats. Effects of chronic angiotensin converting enzyme inhibition. *Circulation* 1991;**83**:1028–1037.
27. Morales C, Rodriguez M, Gonzalez GE, Matoso M, Bertolasi CA, Gelpi RJ. Time course of the myocardial infarction in the rabbit. *Medicina (B Aires)* 2001;**61**:830–836.
28. Smith GT, Soeter JR, Haston HH, McNamara JJ, Coronary reperfusion in primates. Serial electrocardiographic and histologic assessment. *J Clin Invest* 1974;**54**:1420–1427.
29. Geft IL, Fishbein MC, Hashida J, Ninomiya K, Nishizawa S, Haendchen R, Venkatesh N, Rit J, Yano J, Ganz W. Effects of late coronary artery reperfusion after myocardial necrosis is complete. *Am Heart J* 1984; **107**:623–629.
30. Yen K, Vock P, Tiefenthaler B, Ranner G, Scheurer E, Thali MJ, Zwygart K, Sonnenschein M, Wiltgen M, Dirnhofer R. Virtopsy: forensic traumatology of the subcutaneous fatty tissue; multislice computed tomography (MSCT) and magnetic resonance imaging (MRI) as diagnostic tools. *J Forensic Sci* 2004;**49**:799–806.
31. Axel L. Efficient method for selecting cardiac magnetic resonance image locations. *Invest Radiol* 1992;**27**:91–93.
32. Ibrahim T, Nekolla SG, Hornke M, Bulow HP, Dirschinger J, Schomig A, Schwaiger M. Quantitative measurement of infarct size by contrast-enhanced magnetic resonance imaging early after acute myocardial infarction: comparison with single-photon emission tomography using Tc99 m-sestamibi. *J Am Coll Cardiol* 2005;**45**:544–552.
33. Herfkens RJ, Sievers R, Kaufman L, Sheldon PE, Ortendahl DA, Lipton MJ, Crooks LE, Higgins CB. Nuclear magnetic resonance imaging of the infarcted muscle: a rat model. *Radiology* 1983;**147**:761–764.
34. Higgins CB, Herfkens R, Lipton MJ, Sievers R, Sheldon P, Kaufman L, Crooks LE. Nuclear magnetic resonance imaging of acute myocardial infarction in dogs: alterations in magnetic relaxation times. *Am J Cardiol* 1983;**52**:184–188.
35. Garcia-Dorado D, Oliveras J, Gili J, Sanz E, Perez-Villa F, Barrabes J, Carreras MJ, Solares J, Soler-Soler J. Analysis of myocardial oedema by magnetic resonance imaging early after coronary artery occlusion with or without reperfusion. *Cardiovasc Res* 1993;**27**:1462–1469.
36. Krauss XH, van der Wall EE, van der LA, Doornbos J, de Roos A, Matheijssen NA, van Dijkman PR, van Voorthuisen AE, Bruschke AV. Follow-up of regional myocardial T2 relaxation times in patients with myocardial infarction evaluated with magnetic resonance imaging. *Eur J Radiol* 1990;**11**:110–119.
37. McNamara MT, Tscholakoff D, Revel D, Soulen R, Schechtmann N, Botvinick E, Higgins CB. Differentiation of reversible and irreversible myocardial injury by MR imaging with and without gadolinium-DTPA. *Radiology* 1986;**158**:765–769.
38. Karolle BL, Carlson RE, Aisen AM, Buda AJ. Transmural distribution of myocardial edema by NMR relaxometry following myocardial ischemia and reperfusion. *Am Heart J* 1991;**122**:655–664.
39. Krombach GA, Wendland MF, Higgins CB, Saeed M. MR imaging of spatial extent of microvascular injury in reperfused ischemically injured rat myocardium: value of blood pool ultrasmall superparamagnetic particles of iron oxide. *Radiology* 2002;**225**:479–486.
40. Kim RJ, Fieno DS, Parrish TB, Harris K, Chen EL, Simonetti O, Bundy J, Finn JP, Klocke FJ, Judd RM. Relationship of MRI delayed contrast enhancement to irreversible injury, infarct age, and contractile function. *Circulation* 1999;**100**:1992–2002.
41. Steuer J, Bjerner T, Duvernoy O, Jideus L, Johansson L, Ahlstrom H, Stahle E, Lindahl B. Visualisation and quantification of peri-operative myocardial infarction after coronary artery bypass surgery with contrast-enhanced magnetic resonance imaging. *Eur Heart J* 2004;**25**:1293–1299.

42. Fieno DS, Kim RJ, Chen EL, Lomasney JW, Klocke FJ, Judd RM. Contrast-enhanced magnetic resonance imaging of myocardium at risk: distinction between reversible and irreversible injury throughout infarct healing. *J Am Coll Cardiol* 2000;**36**:1985–1991.
43. Farb A, Tang AL, Burke AP, Sessums L, Liang Y, Virmani R, Sudden coronary death. Frequency of active coronary lesions, inactive coronary lesions, and myocardial infarction. *Circulation* 1995; **92**:1701–1709.
44. Jackowski C, Bolliger S, Aghayev E, Christe A, Kilchoer T, Aebi B, Périnat T, Dirnhofer R, Thali M. Reduction of postmortem angiography induced tissue edema by using poly ethylene glycol (PEG) as contrast agent dissolver. *J Forensic Sci* 2005; in print.
45. Scollan DF, Holmes A, Winslow R, Forder J. Histological validation of myocardial microstructure obtained from diffusion tensor magnetic resonance imaging. *Am J Physiol* 1998;**275**:H2308–H2318.
46. Geerts L, Bovendeerd P, Nicolay K, Arts T. Characterization of the normal cardiac myofiber field in goat measured with MR-diffusion tensor imaging. *Am J Physiol Heart Circ Physiol* 2002;**283**:H139–H145.
47. Hsu EW, Muzikant AL, Matulevicius SA, Penland RC, Henriquez CS. Magnetic resonance myocardial fiber-orientation mapping with direct histological correlation. *Am J Physiol* 1998;**274**:H1627–H1634.
48. Chen J, Song SK, Liu W, McLean M, Allen JS, Tan J, Wickline SA, Yu X. Remodeling of cardiac fiber structure after infarction in rats quantified with diffusion tensor MRI. *Am J Physiol Heart Circ Physiol* 2003; **285**:H946–H954.
49. Aghayev E, Thali MJ, Sonnenschein M, Jackowski C, Dirnhofer R, Vock P. Post-mortem tissue sampling using computed tomography guidance. *Forensic Sci Int* 2006; accepted.
50. Jackowski C, Thali M, Aghayev E, Yen K, Sonnenschein M, Zwygart K, Dirnhofer R, Vock P. Postmortem imaging of blood and its characteristics using MSCT and MRI. *Int J Legal Med* 2005;**4**:1–8.